TRANSVERSE AND LONGITUDINAL OPTICAL BEAM DIAGNOSTICS FOR THE BESSY II BOOSTER

M. Marongiu*, P. Ahmels, T. Atkinson, G. Rehm, M. Ries Helmholtz-Zentrum Berlin, Berlin, Germany

Abstract

This paper describes the optical beam diagnostics available at the BESSY II booster synchrotron. For the first time, diagnostics are established to investigate the distribution of the electron beam in all three dimension. A permanent installation of a source-point imaging system aided by a telescope optic depicts the transverse properties of the electron beam. Additionally, the bunch length is measured using a streak camera with a resolution in the picosecond range. Both systems can work in parallel and are able to observe the non-equilibrium beam dynamics over the entire booster ramp.

MOTIVATION

The injector systems and diagnostics were upgraded as part of the global upgrade of the BESSY II facility. Specific for the injector were the E-gun, the bunch-by-bunch feedback, the orbit analysis, additional cavities for acceleration and the diagnostic beamline [1].

The diagnostic beamline transports visible light from a bending magnet out of the tunnel onto an optical table. This mechanical beamline consists of 8 planar mirrors (of which 3 are motorized) and a motorized telescopic lens system. Here, two lenses form an achromatic telescope and help collimate the photon beam for high transmission.

The incentive behind reducing the present bunch length is to optimise beam parameters ready for low-alpha Top-Up operation. For this special optic, the bunch length over the whole booster cycle needs to be carefully diagnosed, controlled and tailored for high injection efficiency into the BESSY II storage ring. Figure 1 shows the development of the photon intensity and with it the bunch length measurement during the injection process.

MECHANICAL BEAMLINE

The beamline uses the synchrotron radiation produced at a predetermined bending magnet. The divergence of the emitted light is corrected using refractive optics. First, the photons are transported through a wedged vacuum window to compensate the angular dispersion and protect the vacuum of the booster. Afterwards, the photons are reflected at a two-inch aluminium mirror into the tunnel system. The beam is collimated via a motorized achromatic telescope system consisting of 400 mm and 80 mm focal length lenses. This system also has a retractable THz detector installed, to study coherent radiation [2].

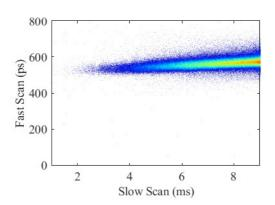


Figure 1: Image captured by the streak camera set with a blanking amplitude of 10 ms (horizontal axis) and the trigger set to observe the injection process.

After the telescope, the collimated beam is transported using the remaining six mirrors (see Fig. 2). Three mirrors are motorized for fine tilt and angle adjustments. An intermediate viewing port (IVP), consisting of a CMOS camera on a motorized linear stage was precautiously installed, to help confirm the alignment of the optical components.

The visible light reaches the optical table with an additional angle of 22° (composed of 2° outcoupled from the bending magnet and 20° due to the building constraints of the tunnel walls).

USER BEAMLINE

After exiting the labyrinth, the beam is reflected through two additional mirrors on to the optical table. The final outcome is three beamline branches: one for source point analysis of the electron beam size, the second for bunch length measurements via a streak camera and finally an R&D beamline for educational purposes [2].

The first branch is the source point analysis system. The beam is transported through a 500 mm achromatic lens mounted on a linear stage for fine-tuning the position and focused on a CCD camera. Presently installed into the setup are three different filters: a polarized filter, a wavelength filter for 550 nm (see Fig. 3) and a ND filter for protection of the camera. The read out of the camera is shown live on a LabVIEW Interface.

On the second branch, a retractable mirror and achromatic Doublet (300 mm) are installed, focusing on a streak camera for bunch length measurements.

^{*} marco.marongiu@helmholtz-berlin.de

Telescope

Source

Optical Table

Figure 2: Schematic of the beamline and the present experimental setup on the optical table.

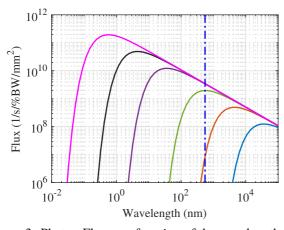


Figure 3: Photon Flux as a function of the wavelength for different electron beam energies. The blue curve represents an energy of 50 MeV, the red 100 MeV, the green 200 MeV, the violet 500 MeV, the black 1 GeV and the magenta 2 GeV. The blue dashed line represents the 550 nm wavelength case.

The R&D beamline provides the possibility for fast diode studies and photon intensity optimisation with a feedback system running on Python [2].

SOURCE-POINT IMAGING

The source-point imaging system works as a high level diagnostic tool for the Booster of BESSY II. It presents live information of the position, the size and the profile in the vertical and horizontal plane of the beam. Important for the system is the high photon intensity in a defined region of interest, Gaussian beam profiles in both planes and beam stability over a long period of time (see Fig. 4).

To optimize the system, three main steps have to be performed in the following order. A good alignment for all mirrors is assumed. The first step is aligning the first two lenses, the telescope, to collimate the beam for high photon transmission. In order to do this, a 2D scan is realized, where the last lens is set near the presumed focus point. This measurement indicates region, where the photon count is maximized on the CCD camera. Simulations with Zemax confirm the optical setup [3]. It is important to note that mainly the relative position to each other is important, rather than the actual position of the lenses in the telescope system.

To further verify the optical configuration of the telescope, a measurement of the photon emittance was undertaken. Comparable to a beam quality factor measurement for a laser, for each telescope setting the final lens was used to scan through the focus at z_0 recording the spot size σ on the camera and determine M^2 given

$$\sigma^{2}(z) = \sigma_{0}^{2} + M^{4} \left(\frac{\lambda}{\pi \sigma_{0}}\right)^{2} (z - z_{0})^{2}, \tag{1}$$

where $\sigma_0^2 = \beta_0 \frac{\lambda}{4\pi}$. This study found M^2 for the horizontal and vertical plane to be 5.3 and 3.3 respectively.

The final characterisation of the source point was to find a balance between staying close to the focus without limiting the resolution due to the pixel size, preserving the Gaussian properties of the beam spot and checking the working point is independent of the polarization. The post-processing algorithm residual from LabVIEW was used to determine the final working point. Here a goal function to minimise the residual product X*Y confirmed the optical configuration of the beamline.

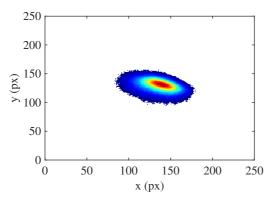


Figure 4: Image captured by the source-point imaging system at the working point (electron beam energy of about 1.7 GeV). The axis scales are in pixels: to convert in mm, one needs to multiply this scale for the pixel size (4.5 μm) and the magnification factor (calculated to be 18).

Once characterized, the configuration for the optical system was in good approximation with the thin lens model, and the magnification factor was calculated to be approximately 18.

The source point imaging system has been found to be an essential diagnostic for daily operation. During an unwanted failure of a magnet power supply, the current in the coils drifted undetected by the electrical diagnostics. This caused a change in the booster orbit below the resolution of the BPM diagnostics and could only be observed at the high resolution imaging system on the optical table. The problem was readily addressed and repaired without any dark time in operation.

BEAM ENVELOPE

For convenience, the electron beam remains in the booster for a full energy cycle without extraction. The beam energy increases on the up ramp to $2\,\text{GeV}$ at $50\,\text{ms}$ and decreases on the down ramp. The diagnostics can then be triggered to characterize the whole $10\,\text{Hz}$ energy ramp.

The measurements consist on the live readout of the horizontal and vertical Gaussian fit results performed while scanning the delay time of the trigger.

The results, showed in Fig. 5, are in good agreement with the theoretical expectation with the horizontal size that grows from 1.5 mm to 1.7 mm (2 mm at 2 GeV without extraction) while the vertical size decrease from 0.7 mm to 0.4 mm (and then grows again to 0.7 mm).

For delay time below 20 ms, the results are not reliable due to the limited dynamic range of the camera. Also, in order to avoid saturation at high energies, a ND filter has been used, this then needs to be removed for low energy measurements.

Streak Camera

The study of the longitudinal properties of an electron beam in a synchrotron machine is typically done with a streak camera. One parameter (the so-called "Time Range")

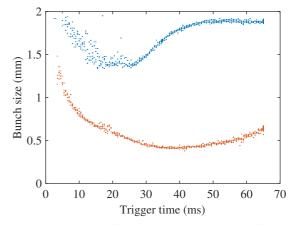


Figure 5: Evolution of the bunch transverse profile in the booster. The blue dots represent the horizontal profile, while the reds dot the vertical one.

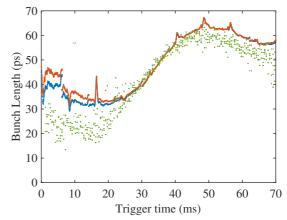


Figure 6: Evolution of the bunch length in the booster. The blue dots represent the Gaussian fit, the red dots represent the skew-normal fit, while the green dots represent the live readout (FWHM divided by 2.355 for comparison).

controls the fast scan and, hence, the bunch length resolution (and field of view). Another parameter (the "blanking amplitude") controls the slow scan, and it is therefore useful to determine the time window of observation: for instance, a small blanking amplitude like $100\,\mathrm{ns}$ allows to view the individual bunches, a value in the $\mu\mathrm{s}$ range allows to view multiple turns while a larger value (ms) allows to observe long range phenomena like the ramp up in electron-beam energy.

In a similar manner as above, the delay trigger can be scanned for the longitudinal studies. The streak camera was set to a Blanking Amplitude value of 10 ms: that means that each image shows a 10 ms evolution of the beam with the trigger delay value as a starting time. The measurement has been performed in single bunch configuration; this is due to the fact that in the high charge multi-bunch configuration (5 mA), electron beam instability is observed at lower energies. This makes the proper characterization of the injection phase challenging.

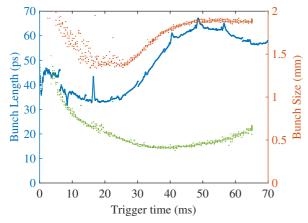


Figure 7: Electron-beam envelope in the booster: the longitudinal envelope is plotted in blue (left scale in ps) while the horizontal and vertical envelopes are plotted in red and green, respectively (right scale in mm).

At first, the measurements were performed through the Hamamatsu native software that allows to remotely store the calculated FWHM in a specific ROI; however, this method is not robust and reliable when the Signal to Noise Ratio (SNR) becomes too low. This condition happens in the first bunch-turns in the booster when the electron energy is still close to the initial value of 50 MeV.

Therefore, an offline analysis has also been performed: images at different trigger delay have been saved and later analysed both evaluating the FWHM and by means of a Gaussian Fit (see Fig. 6).

It can be seen from Fig. 6 that for electron energy below 100 MeV (trigger time of 25 ms), the Gaussian fit and the Hamamatsu evaluation diverges and the latter is no longer reliable.

Furthermore, it should be also point out that in the first turns the electron bunch profile is not purely Gaussian, but it presents some asymmetry (close to a triangular profile): different fit functions rather than the Gaussian has been studied (i.e. skew-normal). The fit is improved from 0.9 to 0.92 (about 2 %) in the first 20 ms, and the corresponding bunch length is increased by 8 %. After this time, the two results do not differ significantly (less than 1 %).

Finally, in Fig. 7 the evolution in time of the bunch size in all the three planes is reported.

OUTLOOK

The beamline was brought into operation through careful planning without any dark time. Recently, the refractive optic was installed and alignment is continually ongoing. A full characterization of the source-point imaging is part of a B.Sc. thesis [3].

These improvements in the beamline were useful to perform a time resolved analysis of the bunches as they get accelerated in the booster before entering the storage ring.

The source-point imaging was used to study the transverse beam dynamics during the booster ramp, finding a good agreement with theoretical expectation.

A streak-camera was used to study the longitudinal evolution during the ramp: the best results have been obtained with an offline analysis and a skew-normal fit due to the asymmetric particle distribution at low energy (at the beginning of the ramp).

A fast live-mode scan was also implemented with the streak-camera, and with the source-point imaging as well, but this shows unreliable results for low energies (below 100 MeV) when the SNR is too low.

This is the first time that such a diagnostic tool has been used to show the evolution of the beam during a booster ramp. The facility now has the key-components to tailor beams from the pre-injector to the electron storage ring, preserving the high injection efficiency.

REFERENCES

- T. Atkinson *et al.*, "Status and prospects of the BESSY II injector system", in *Proc. IPAC'16*, 2016. doi:10.18429/JACOW-IPAC2016-WEPOW007
- [2] P. Ahmels *et al.*, "Research and development beamline for the BESSY II Booster", presented at IBIC'24, Beijing, China, Sep. 2024, paper THP54, this conference.
- [3] P. Ahmels, "Inbetriebnahme des Aufbaus eines optischen Messinstruments zur Quellpunktabbildung am Vorbeschleuniger von BESSY II", Bachelor Thesis, Technical University Berlin, Berlin, Germany, 2023.